2009 International Nuclear Atlantic Conference - INAC 2009
Rio de Janeiro,RJ, Brazil, September27 to October 2, 2009
ASSOCIAÇÃO BRASILEIRA DE ENERGIA NUCLEAR - ABEN
***ISBN:* 978-85-99141-03-8**

RECONSTRUCTION OF SEGMENTED HUMAN VOXEL PHANTOMS FOR SKIN DOSIMETRY

Paula C. G. Antunes[1,*], Paulo de Tarso D. Siqueira[1], Hélio Yoriyaz[1], Gabriel P. Fonseca[1] Gabriela Reis[2] and Laura Furnari[2]

[1] Instituto de Pesquisas Energéticas e Nucleares, IPEN - CNEN/SP
Av. Professor Lineu Prestes, 2242
05508-000, São Paulo, SP
pacrisguian@usp.br
ptsiquei@ipen.br
hyoriyaz@ipen.br
gabriel.fonseca@usp.br

[2] Serviço de Radioterapia do Instituto de Radiologia do Hospital das Clínicas de São Paulo.
Av. Dr. Enéas de Carvalho Aguiar, 255
05403-900, São Paulo, SP
reis.gabby@gmail.com
laurafurnari@hotmail.com

ABSTRACT

High-resolution medical images along with methods that simulate the interaction of radiation with matter, as the Monte Carlo radiation transport codes, have been widely used in medical physics procedures. These images provide the construction of realistic anatomical models, which after being coupled to these codes, may drive to better assessments of dose distributions on the patient.
These anatomical models constructed from medical images are known as voxel phantoms (voxel - volume element of an image). Present day regular images are unsuitable to correctly perform skin dose distribution evaluations. This inability is due to improper skin discrimination in most of the current medical images, once its thickness stands below the resolution of the pixels that form the image.
This paper proposes the voxel phantom reconstruction by subdividing and segmentating the elements that form the phantom. It is done in order to better discriminate the skin by assigning it more adequate thickness and actual location, allowing a better dosimetric evaluation of the skin. This task is an important issue in many radiotherapy procedures. Particular interest lays in Total Skin Irradiation (TSI) with electron beams, where skin dose evaluation stands as the treatment key point of the whole body irradiation. This radiotherapy procedure is under implementation at the Hospital das Clínicas da Universidade de São Paulo (HC-USP).

1. INTRODUCTION

Computer systems have been incorporated in medical physics procedures in order to assist the development of adequate planning systems through the calculation of the patient dose distribution.

Monte Carlo techniques have been widely used to provide very useful information and more accurate results through the simulation of radiation transport [1].

This is mainly due to their capability to perform radiation transport calculations, even for highly detailed geometrical systems. Therefore, rather than solving transport equations in quite limited applicable systems, Monte Carlo based transport codes simulate the interaction of radiation with matter, using statistical methods in order to sort physical phenomena and to quantify selected physical parameters.

The accuracy of the data obtained by these codes, is directly associated with their possibility to geometrically describe the object of study in a highly detailed way, therefore providing more realistic representation of system under study. Medical images obtained either from Computer Tomography (CT) or Magnetic Resonance Imaging (MRI) stand as the most adequate data set to geometrically describe a patient, and have, therefore, been used as the basic data for the construction of segmented phantoms [2].

The resolution of the segmented phantom, i.e. the degree in which the human body may be geometrically represented in the simulation, is directly related to the medical images resolution, which is around 3-4 mm for most of the available machines. Such resolution, however, limits depicting some fine structures of the human body, such as the skin, which has an average thickness of approximately 1.5 mm [3].

Skin dosimetry is a demand of both radioprotection and radiotherapy areas as skin is the largest organ of the human body, making up 15 to 16 % of the body weight, practically covering the whole body surface [3]. Skin extent, width and distribution turn Monte Carlo radiation transport method in the ideal approach to perform skin dose distribution evaluation as long as it can be correctly represented in the simulating system.

This work intends to present the approach used to overcome the unfeasibility to take the advantage of the Monte Carlo based radiation transport codes to perform skin dosimetry. As there is no sufficient image resolution to properly characterize the skin by the mentioned medical image resolution, a computational routine has been created to divide and segment the voxels that represent the skin in the segmented voxel phantoms.

Such phantoms should differentiate the skin, assigning it adequate thickness allowing the correct modeling of the system. Subsequently, an adequate simulation aiming at the evaluation of the dose distribution in the skin can be performed.

2. MATERIALS AND METHODS

2.1. MCNP - A general Monte Carlo N-Particle transport code

MCNP code stands out as one of the most distinguished Monte Carlo based radiation transport codes. The program is suited to simulate interactions of photons, electrons, and neutrons with matter throughout an user-defined problem geometry and material compositions. Its design enables the simulation of wide sort of problems, where the general source definition and geometrical specification stand out [1].

Repeated structure is an important feature of this code, in which regular geometric structures may be defined many times with relatively simple input statements. It is possible to simulate

radiation transport in very complex and heterogeneous geometric structures, including even discontinuous regions such as those found in the human body.

This resource is based on the definition of unit structures using the concept “cells”, (volume elements defined by the combination of surfaces predefined in the code). A cell is defined only once with possible repetitions throughout the geometric modeling [1]. This procedure creates a sequence of cells that form a two- or three-dimensional discrete array according to given geometric information of the problem to be solved.

2.2. Voxel Model

Medical images obtained by Computer Tomography (CT) or by Magnetic Resonance Imaging (MRI) are two-dimensional representations of body anatomic structures depicted by picture/image elements called pixels. Each image is a matrix of pixels to which specific parameter values, such as gray tones, are assigned. The amount of elements arranged in a matrix is straightly related to the resolution of the equipment used for the image acquisition [2].

A consecutive set of such images can be considered as a three-dimensional matrix made of voxels (volume pixels), called voxel model. This model is a realistic representation of the human body in three-dimensions.

Voxel models were introduced by Gibbs [4] and also by Williams [5], independently. Since then, several models were created representing man, woman and child, using data obtained from Reference Man [3] as MAX [6], FAX [7], Zubal [8], among others.

2.3. Phantom Segmentation

Segmentation is the initial phase of an image processing. It consists of subdividing a region in parts or objects according to similar features among them, i.e. an image in pixels/voxels representing the same region and having characteristics in common, when segmented, are represented by identical values of identification (ID), allowing the identification of structures and detection of regions of interest from the homogenization of ID's [9].

The segmentation of a voxel phantom to discriminate the skin was achieved using the following methodology:

- Phantom homogenization and classification per region;
- Detection of voxels which constitute the skin;
- Classification of voxels which compose the skin according to their localization.

These processes are described in detail throughout sections 2.3.1 to 2.3.3.

The proposed methodology may be directly applied to medical images (figure 1a), or to voxel models constructed in MCNP input files (figure 1b). However, in this instance, MCNP input file shall go through a pre-processing procedure is order to convert MCNP voxel model format to a matrix of pixel/voxel.

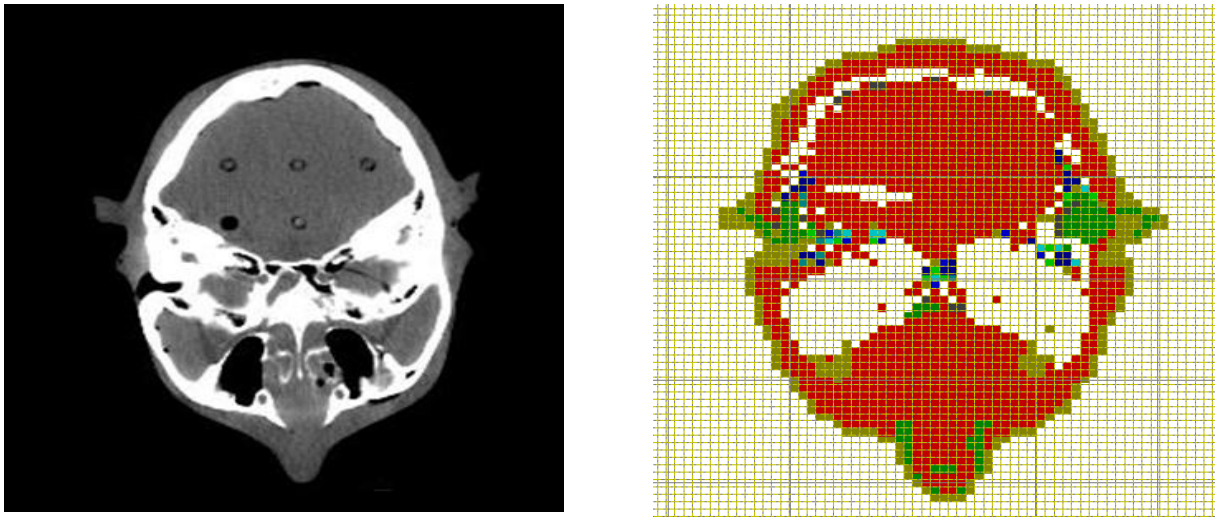

Figure 1. Possible data of the proposed methodology. A) Axial slices of a tomography image. B) Axial slice of a voxel phantom.

This procedure converts the voxel model described in MCNP input into a matrix (figure 2), making the same methodology of skin discrimination possible to be used not only for images, but also for MCNP input file.

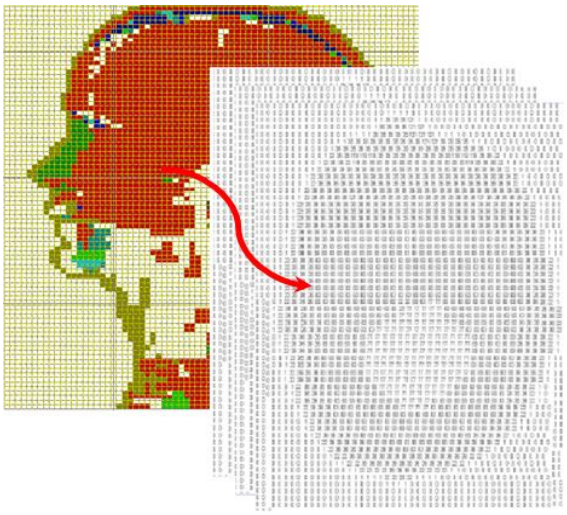

Figure 2. Voxel phantom converted to the format of a matrix of pixel.

In the following sections, a methodology for the segmentation of a 2D matrix will be described. However, the same methodology was used for 3D matrices by assigning an extra dimension (thickness) to pixels of the tomographic images.

2.3.1. Matrix Homogenization

The image homogenization was done by a mathematical algorithm constructed from the simplified technique of threshold segmentation [9].

This technique is based on the similarity of the pixels; with a threshold *t* used to classify at which region one pixel belongs. To each *n* values of the threshold, the image is divided in *n*+1 regions. With a single threshold *t*, the image is divided in two regions, A and B, like the equations 1 and 2.

$$S(x, y) \leq t \rightarrow (x, y) \in A \tag{1}$$

$$S(x, y) > t \rightarrow (x, y) \in B \tag{2}$$

Where, $S(x, y)$ is the intensity of a pixel in the position (x, y). Each pixel is then analyzed according to equations 1 and 2 and it is determined whether the pixel belongs to the image or not, according to threshold t. Pixels belonging to the same region receive identical ID values, originating homogeneous regions.

2.3.2. Edge detection

In order to perform the edge detection, a mathematical algorithm that analyzes the neighbourhood of the pixels [9] was applied to the matrix. In this algorithm, all possible connections of each pixel belonging to the image (region A) is checked according to Equation 3.

$$if\ ((x+1, y) \wedge (x-1, y) \wedge (x, y+1) \wedge (x, y-1)) \in B \rightarrow (x, y) \in C \tag{3}$$

Where, the symbol "$\wedge$" stands for "OR". This equation evaluates the 4 possible - N4(S) – next neighbour connections of a pixel that belongs to core of the image (region A). Whenever one or more connected pixel belongs to region B, this pixel is assigned to region C, region that represents the skin.

From this analysis, matrix pixels are arranged/segmented in 3 distinct regions:

- A - core of the image;
- B - background (pixels which do not take part of object under study);
- C - edge (image elements that stands next to B).

2.3.3. Edge classification

The classification of pixels which take part of the edge region is necessary for the proper skin modeling, because one must know the accurate location of the skin in a pixel/voxel so to model the skin closer to reality.

As the skin thickness is below pixel sizes, it shall represent only a part of a pixel. Where around and how much of a pixel it takes place depends on its classification.

In one pixel there are 14 possible combinations for the location of the skin (4 1-pixel-edge skin, 6 2-pixel-edge skin and 4 3-pixel-edge skin). In one voxel, this number increases to 62 combinations. In order to discriminate the localization of the skin, a new mathematical algorithm, similar to the one proposed in section 2.3.2, was built. However, the goal of this new algorithm is to reclassify the pixels of the edge region according to the possible combinations of the skin location assigning a new ID value for each possible combination, as exemplified by equation 4.

$$if\ (\{[(x-1,y)\vee(x,y+1)]\in B\}\vee\{[(x+1,y)\vee(x,y-1)]\in A\})\rightarrow ID(x,y)=21 \qquad (4)$$

Where, the symbol "$\vee$" means "AND". Equation 4 evaluates for each pixel, the region of neighboring pixels. If its upper neighbour and its left neighbour belong to B, and its lower neighbours and its right neighbour belong to A. The pixel C(x,y) is assigned an ID 21, which represents the connection outlined in Figure 3.

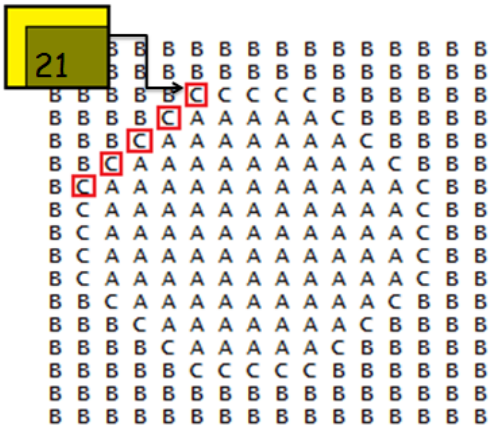

Figure 3. Schematic representation of the skin classification algorithm in two-dimensions: pixels that represent the skin are further discriminated by associating an ID value according to their relative location on the image.

This discrimination is done pixel by pixel, attributing to each pixel of the edge an ID value associated to the skin location in the pixel. From this reclassification, it is possible to reconstruct the phantom depicting the skin with its skin thickness closer to reality.

3. RESULTS AND DISCUSSION

3.1. Phantom Reconstruction

This methodology was applied to a 56.88 cm wide (x), 26.64 cm thick (y), and 32.4 cm height (z) head-neck voxel phantom (Figure 2). Originally, this phantom discriminated internal organs and was comprised of 90 axial slices, each of them made of 11,691 0.36x0.36x0.36 cm^3 voxels, summing up 1,052,190 voxels.

Two different phantom reconstructions were carried out. Homogenization and edge detection, as proposed in sections 2.3.1 and 2.3.2, were performed for both reconstructions and voxels were discriminated into 3 categories: image, background and edge, as mentioned before. Difference between reconstructed phantoms lays on the skin characteristic thickness by assigning a whole voxel volume to each edge voxel (figure 4a) or by applying the edge voxel subdivision and segmentation as proposed in section 2.3.3 (figure 4b). Skin thicknesses were then assigned the following values for the forementioned reconstructed phantoms: 3.6 mm and 1.5 mm, respectively. These phantoms were properly inserted into MCNP input files together with characteristics material compositions and densities.

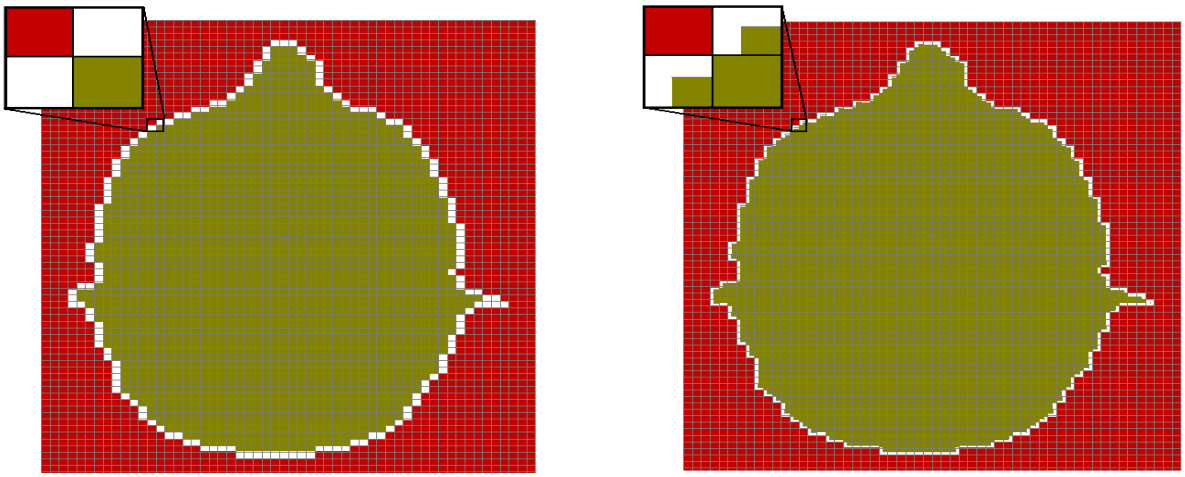

Figure 4. Axial slice obtained by the MCNP plot command representing homogenized segmented voxel phantom with skin segmentation, for two different thicknesses. A) 3.6 mm skin represented by an entire voxel. B) 1.5 mm skin represented by parts of voxel.

3.2. Dose Distributions in the Voxel Phantom

These phantoms were properly inserted into an MCNP input file together with characteristics material compositions and densities. Simulations, here shown, were however carried out for

only one slice of each phantom. A source 4 MeV monoenergetic photon source was placed 5 cm to the left of the left ear.

A hundred million photon histories were simulated, obtaining an analytical point of energy deposited per gram (dose) in each cell. Figure 5left shows a dosimetric distribution of non-segmented voxels (Figure 4a phantom) and, Figure 5right with voxels subdivided (Figure 4b phantom).

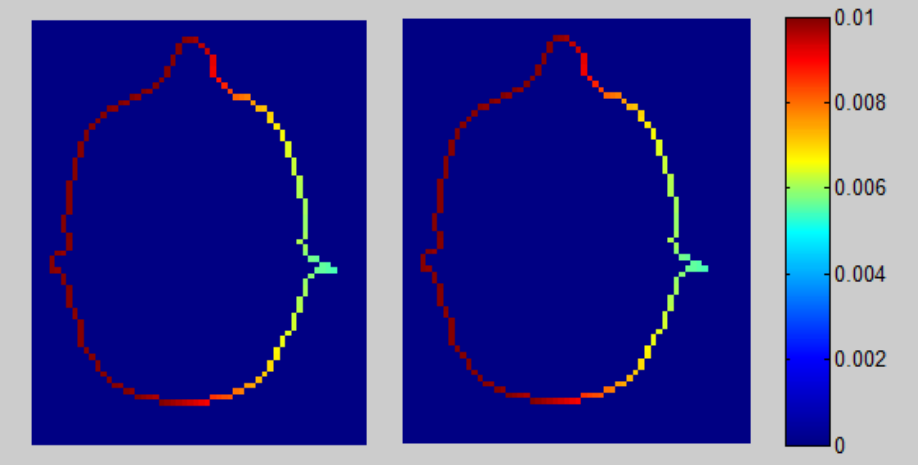

Figure 5. Skin Dose Distribution of photon source on axial slice. Left) Dose Distribution from Figure 4a. Right) Dose Distribution from Figure 4b.

Figure 5 shows similar dose distributions for the 2 considered phantoms. It was expected, as the photon dose profile does not show any significant changes in the order of a voxel length.

On the other hand, as electron dose profiles do present completely different pattern, showing high dose gradients, it is expected to get different skin dose distribution estimates from these phantoms. Due to a larger simulation time demand to perform electron transportation by Monte Carlo method, it has not been possible to provide any electron beam simulation.

This variation in total and punctual dose becomes a very significant effect for an electron beam study case, because electrons are short range particles, with limited penetration, and have therefore, a more pronounced variation on its depth dose profile than do photon

The results obtained so far for photon beam validate and illustrate the proposed methodology, obtaining expected results, with very small percentage errors, less than 0.5%. The importance of this methodology will be emphasized in simulations of electron beam treatments, where the voxel size becomes an extremely important factor.

4. CONCLUSIONS

The methodology proposed in this work stands as a valuable tool for voxel phantom reconstruction, providing proper skin discrimination and better suiting it to be coupled to Monte Carlo radiation transport codes

This methodology will be better detailed in the future, so to consider all possible connections for each pixel, taking into account the diagonal neighbour voxels rather than limiting edge detection and classification to the side by side neighbours check. This is expected to lead to more precise skin dose evaluations.

Simulations carried out with photons resulted in the expected outcomes validating the proposed methodology. It is believed that problems involving electron beam dosimetry shall derive more precise and intriguing results as the electron shows a pronounced dose gradient profile. Such simulations are under progress and will be presented in later works.

Skin dosimetry assessment by Monte Carlo simulation is a new and very significant evaluation methodology for several radiotherapy procedures, mainly in the service of Radiotherapy of Hospital das Clínicas da Universidade de São Paulo (HC-USP).

ACKNOWLEDGMENTS

The authors acknowledge CNPq for supporting one of the authors (*).

REFERENCES

1. X-5 Monte Carlo Team, *MCNP – A general Monte Carlo N-Particle transport code*, Version 5, Los Alamos National Laboratory Report, LA-CP-03-0245 (2003).
2. H. Yoriyaz, M. G. Stabin and A. Santos, "Monte Carlo MCNP-4B-Based Absorbed dose Distribution Estimates for Patient-Specific dosimetry," *J. Nucl. Med*, **Vol.42**, No.4, pp.662-69 (2001).
3. International Commission on Radiological Protection, *Basic Anatomical and Physiological Data for Use in Radiological Protection: Reference Values 89*, Annals of ICRP, Series 89 (2002).
4. S. J. Gibbs, A. Pujol, T. S. Chen, A. W. Malcolm and A. E. James, "Patient risk from interproximal radiography," *Oral Surg. Oral Med. Oral Pathol.*, **Vol.58**, pp.347-54 (1984).
5. G. Williams, M. Zankl, W. Abmayr, R. Veit and G. Drexler, "The calculation of dose from external photon exposures using reference and realistic human phantoms and Monte Carlo methods," *Phys. Med. Biol.*, **Vol.31**, pp.347-54 (1986).
6. R. Kramer, J. W. Vieira, H. J. Khoury, F. R. A. Lima and D. Fuelle, "All about MAX: a male adult voxel phantom for Monte Carlo calculations in radiation protection dosimetry," *Phys. Med. Biol.*, **Vol.48**, pp.1239-62 (2003).
7. R. Kramer, H. J. Khoury, J. W. Vieira, E. C. M. Loureiro, V. J. M. Lima, F. R. A. Lima and G. Hoff, "All about FAX: a female adult voxel phantom for Monte Carlo calculations in radiation protection dosimetry," *Phys. Med. Biol.*, **Vol.49**, pp.5203-16 (2004).

8. G. Zubal, C. Harrel, E. Smith, Z. Ratner, G. Gindi and P. Hoffer, "Computerized three-dimensional segmented human anatomy," *Med. Phys.*, **Vol.21**, pp.299-302 (1994).
9. R. C. Gonzalez, and R. E. Woods, *Digital Image Processing*, Second edition, Prentice Hall (2002).